AD-A097 195 AERONAUTICAL RESEARCH LABS MELBOURNE (AUSTRALIA) F/G 1/3
STRUCTURAL DESIGN OF BFRP PATCHES FOR MIRAGE WING REPAIR.(U)
JUL 80 R JONES, R J CALLINAN

UNCLASSIFIED ARL/STRUC-NOTE NL

END
DATE
FILMED
DTIC

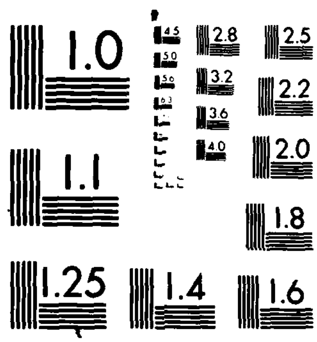

MICROCOPY RESOLUTION TEST CHART
NATIONAL BUREAU OF STANDARDS-1963-A

ARL-STRUC-NOTE-461 LEVEL (12) AR-002-214

AD A097195

DEPARTMENT OF DEFENCE

DEFENCE SCIENCE AND TECHNOLOGY ORGANISATION

AERONAUTICAL RESEARCH LABORATORIES

MELBOURNE, VICTORIA

STRUCTURES NOTE 461

STRUCTURAL DESIGN OF BFRP PATCHES FOR MIRAGE WING REPAIR

by

R. JONES and R. J. CALLINAN

Approved for Public Release.

COPY No 17

JULY 1980

AR-002-214

DEPARTMENT OF DEFENCE
DEFENCE SCIENCE AND TECHNOLOGY ORGANISATION
AERONAUTICAL RESEARCH LABORATORIES

STRUCTURES NOTE 461

STRUCTURAL DESIGN OF BFRP PATCHES FOR MIRAGE WING REPAIR

by

R. JONES [redacted] R. J. CALLINAN

SUMMARY

This paper is concerned with the design aspects of two repair schemes developed for application to the lower wing skin of Mirage aircraft. Both repairs involve bonding a boron fibre reinforced plastic (BFRP) patch to the wing skin. In one instance the skin is cracked and the patch is acting as a crack stopper, while in the other instance the patch covers a series of holes and its prime purpose is to lower the stress field.

POSTAL ADDRESS: Chief Superintendent, Aeronautical Research Laboratories,
Box 4331, P.O., Melbourne, Victoria, 3001, Australia.

DOCUMENT CONTROL DATA SHEET

Security classification of this page: Unclassified

1. Document Numbers (a) AR Number: AR-002-214 (b) Document Series and Number: Structures Note 461 (c) Report Number: ARL-Struc-Note-461	2. Security Classification (a) Complete document: Unclassified (b) Title in isolation: Unclassified (c) Summary in isolation: Unclassified

3. Title: STRUCTURAL DESIGN OF BFRP PATCHES FOR MIRAGE WING SKIN REPAIR

4. Personal Author(s): R. Jones and R. J. Callinan	5. Document Date: July, 1980 6. Type of Report and Period Covered:
7. Corporate Author(s): Aeronautical Research Laboratories 9. Cost Code: 21 1245	8. Reference Numbers (a) Task: Air 78/041 (b) Sponsoring Agency: Dept. of Defence (Air Force Office)
10. Imprint Aeronautical Research Laboratories, Melbourne	11. Computer Program(s) (Title(s) and language(s)):

12. Release Limitations (of the document)
Approved for public release

12-0. Overseas:	N.O.		P.R.	1	A		B		C		D		E	

13. Announcement Limitations (of the information on this page):
No limitations

14. Descriptors:		15. Cosati Codes:
Mirage aircraft	Maintenance	1104
Fiber composites	Boron reinforced	1109
Reinforced plastics	materials	

16. *ABSTRACT*

This paper is concerned with the design aspects of two repair schemes developed for application to the lower wing skin of Mirage aircraft. Both repairs involve bonding a boron fibre reinforced plastic (BFRP) patch to the wing skin. In one instance the skin is cracked and the patch is acting as a crack stopper, while in the other instance the patch covers a series of holes and its prime purpose is to lower the stress field.

CONTENTS

1. INTRODUCTION

In the course of establishing an extended life of type for the Mirage III in service with the Royal Australian Air Force a full scale fatigue test was carried out at the Aeronautical Research Laboratories in 1974. Since the complete airframe could not be obtained the fatigue test was conducted on a wing as this had been predicted to be the most fatigue critical item. Although final failure occurred in the main spar severe cracking also occurred at the fairing attachment hole in the lower wing skin, closest to the main spar. As a direct result of the cracking of the skin the Aeronautical Research Laboratories were tasked with the development of a precautionary boron fibre reinforced plastic (BFRP) patch for possible application to the wing skin in this region.

Fatigue cracks were later discovered around the fuel decant hole in the lower wing skin of Mirage aircraft in service with the RAAF. As a result, after consultation with the RAAF, a BFRP field repair was developed by ARL for this area. Because of the significance of the cracking and the long life required of the repairs a considerable amount of research and development was required before the repairs could be implemented. This paper deals primarily with the design of the two repair schemes, which was based on a finite element study. Other aspects of these repairs are discussed, for example, in the paper by Baker *et al.* [1].

2. BASIC THEORY

In developing fibre composite repair schemes (i.e., patches) for application to aircraft it is particularly important that a realistic model be used for the shear stress developed in the adhesive layer bonding the patch to the structure. The model developed by the authors in [2, 3] is given below for the specific case when the x_y axis system coincides with the axes of orthotropy of the patch, viz:

$$\tau_{sx} = (u_0 - u_s) \Big/ \left(\frac{t_a}{G_a} + \frac{3t_s}{8G_s} + \frac{3t_0}{8G_{13}}\right)$$

$$\tau_{sy} = (v_0 - v_s) \Big/ \left(\frac{t_a}{G_a} + \frac{3t_s}{8G_s} + \frac{3t_0}{8G_{23}}\right)$$

Here τ_{sx} and τ_{sy} are the shear stresses developed in the adhesive, t_a, t_s and t_0 are the thicknesses of the adhesive, sheet and patch respectively, (u_0, v_0), (u_s, v_s) are the (x, y) displacements in the patch and the sheet, G_s and G_a are the shear moduli of the sheet and the adhesive while G_{13} and G_{23} are the transverse shear moduli of the patch.

The terms $1 \Big/ \left(\frac{t_a}{G_a} + \frac{3t_s}{8G_s} + \frac{3t_0}{8G_{13}}\right)$ and

$1 \Big/ \left(\frac{t_a}{G_a} + \frac{3t_s}{8G_s} + \frac{3t_0}{8G_{23}}\right)$ may be

---

1. A. A. Baker, R. J. Callinan, M. J. Davis, J. G. Williams and R. Jones, Application of BFRP crack patching to Mirage III aircraft, Proceedings 3rd ICCM, Paris, France, 1980. (In press).

2. R. Jones, and R. J. Callinan, Finite Element analysis of patched cracks, J. of Structural Mechanics, 7, 2, pp. 107–130, 1979.

3. R. Jones, and R. J. Callinan, Developments in the analysis and repair of cracked and uncracked structures, Proceedings 3rd Int. Conf. in Australia on Finite Element Methods. Sydney, July 1979, pp. 231–245.

regarded as spring constants and for typical repairs differ by 40–50% from the simplistic approximation of G_a/t_a used by other investigators [4, 5].(See [2] for further details). The effect of this error on the stiffness matrix for the structure is to overestimate the stiffness of the adhesive layer. However, as shown in [2, 6], this has little effect on the efficiency of the patch, (e.g. on the reduction in the stress intensity factor). But the simplistic model drastically overestimates the shear stress in the adhesive. This is not important in lightly loaded areas, but for repairs to areas which carry a substantial amount of load it would often mean the unnecessary rejection of the concept of a fibre reinforced plastic patch.

This point is particularly important in the present investigation since the wing skin in the vicinity of the spar and root rib is heavily loaded. For experimental work of direct relevance to the above, readers are referred to References [1, 7].

3. REPAIR TO THE FAIRING ATTACHMENT HOLE REGION

Following the development of cracks at the fairing attachment hole in the lower wing skin during the ARL fatigue test on the Mirage III aircraft, ARL was tasked with the development of a precautionary fibre reinforced plastic patch. A finite element model of the area surrounding the fairing attachment hole was developed; see Figure 1. This model consisted of 359 quadrilateral membrane elements and 155 constant strain triangular elements representing the wing skin, which is 3·39 mm thick, and 21 flange elements representing the integrally milled stiffeners.

The stress distribution in the panel was obtained from the loading shown in Figure 2. This was adjusted to give results that agree with strain gauge readings, obtained from the ARL test, near the fairing hole of:

$$\sigma_1 = 131 \text{ MPa}, \quad \sigma_2 = -64 \text{ MPa}$$

where σ_1 and σ_2 are the principal stresses and where the σ_1 stress is at an angle of 33 degrees to the spar. This reading occurred when the load on the wing, in the test, was representing a 6g flight manoeuvre load. The strain gauge reading is particularly relevant since the crack at the fairing hole was at an angle of 147 degrees to the spar. Using the criterion that cracks grow perpendicular to the maximum principal stress this reveals that the principal stress field was indeed 33 degrees to the spar as indicated by the strain gauge reading.

On the basis of this information a complex distribution of loads (see Fig. 2) was applied to the edges of the model for the wing skin panel shown in Figure 1. This load distribution gave the principal stresses at the strain gauge location in the test as

$$\sigma_1 = 124 \text{ MPa}, \quad \sigma_2 = -84 \text{ MPa}.$$

at an angle of 34 degrees to the spar. These stresses compare reasonably with those measured for the 6g load case.

Let us now turn our attention to the stress distribution at the fairing attachment hole and the associated two rivet holes. The finite element model gave the maximum stresses at the holes to be at the points labelled 1, 2, 3, 4, 5 and 6 in Figure 1. The principal stresses at these locations are shown in Table 1 as is the angle that the maximum principal stress makes with the spar.

4. K. Arin, A plate with a crack stiffened by a partially debonded stiffener, Engng. Frac. Mech. 6, pp. 133–140, 1974.

5. K. Arin, A note on the effect of lateral bending stiffness of stringers attached to a plate with a crack, Engng Frac. Mech, 7, pp. 173–179, 1975.

6. R. Jones, and R. J. Callinan, A design study in crack patching. Aeronautical Research Laboratories. Structures Report No. 376, 1979.

7. R. A. Mitchell, R. M. Wooley and D. J. Chivirut, Analysis of composite reinforced cutouts and cracks, AIAA, 13, pp. 744–749, 1975.

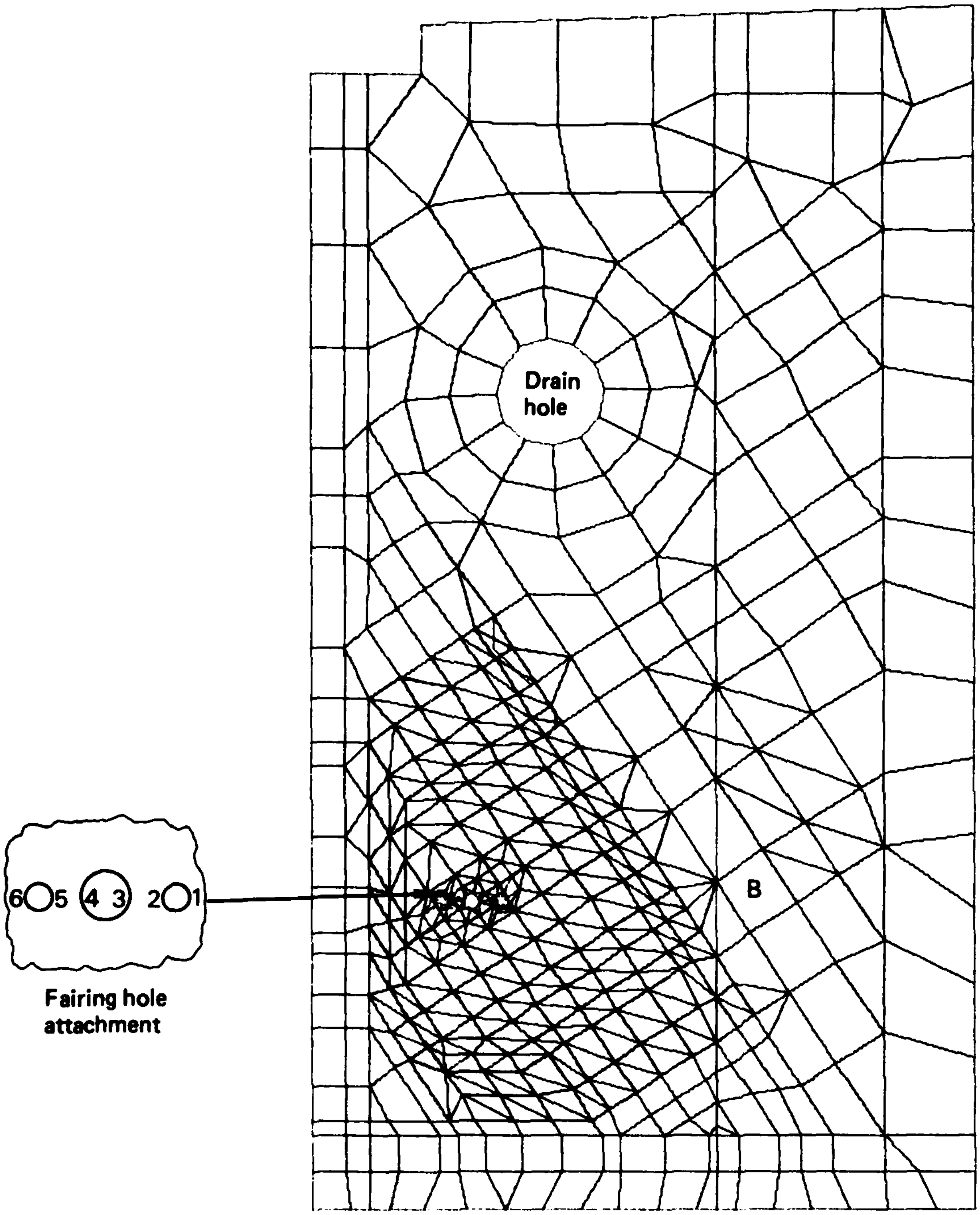

FIG. 1 FINITE ELEMENT MODEL OF FAIRING HOLE REGION

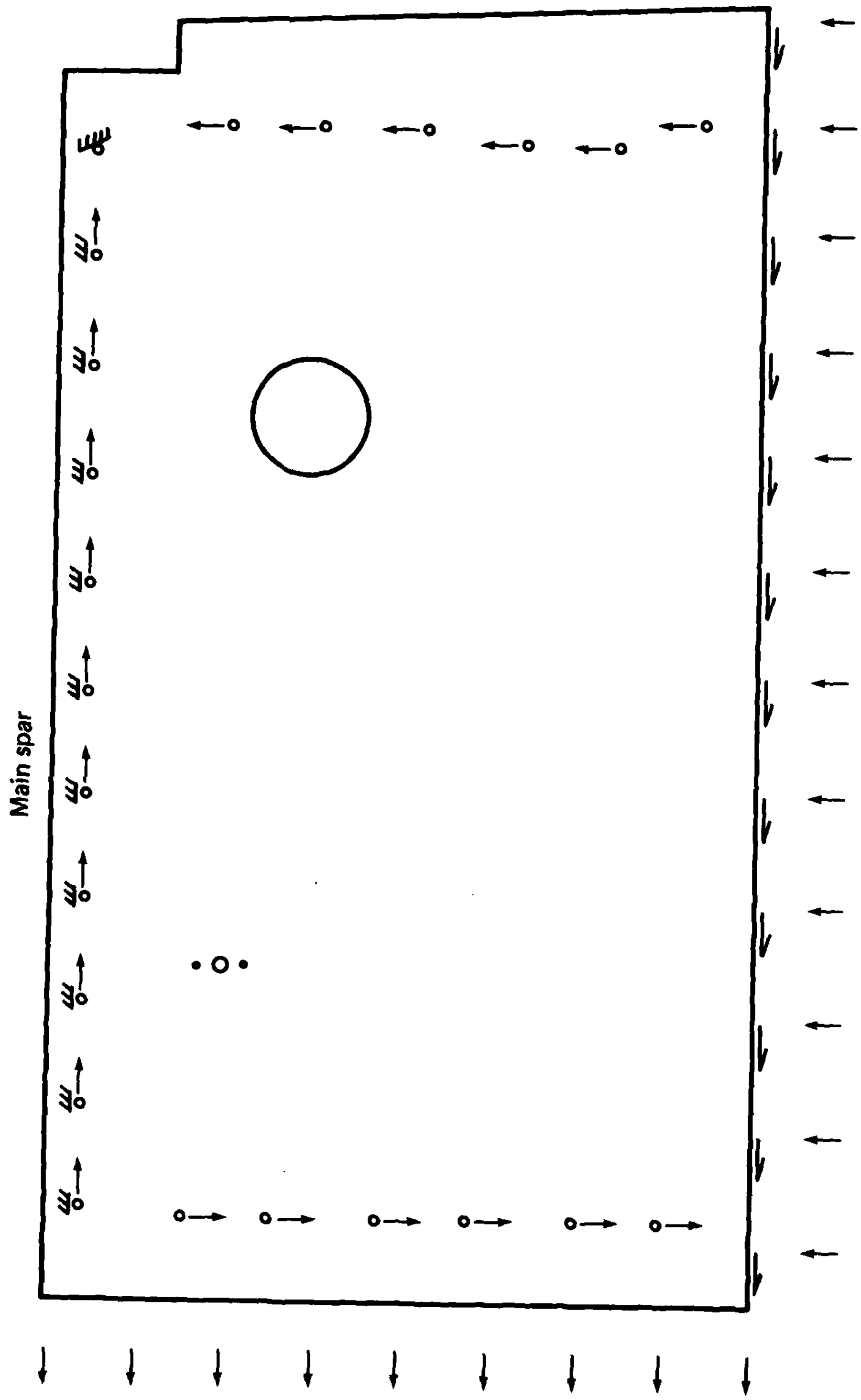

FIG. 2 LOAD DISTRIBUTION APPLIED TO PANEL

TABLE 1

Principal Stresses (MPa) in Fairing Attachment Hole Regim

Location	σ_1	σ_2	Angle from Spar (degrees)
1	202	−32	36
2	208	−71	34
3	207	−64	34
4	194	−42	32
5	194	−79	35
6	194	−37	34

From this table we see that the maximum principal stress occurs at location 2 and is at 34 degrees to the spar. It is interesting to note that, as mentioned before, this angle coincides with that required for the observed angle of the crack in the ARL test. It is also interesting to note that a fractographic investigation of the crack in the test has also indicated that cracking initiated at location 2.

However although location 2 is the point of maximum stress there is very little difference between the stresses at locations 1, 2 or 3. As a result any slight imperfection or change in the nature of the load on the wing could easily cause crack initiation at any of the locations 1, 2 or 3. This is particularly important since it is a possible explanation of why cracking in the wing skin in the ARL fatigue test of the Mirage III started at location 2 whereas cracking in the Swiss fatigue test of the Mirage III started at location 3. In both tests the angle of the crack to the spar was approximately the same.

Having thus obtained a reasonable model for the unpatched wing skin we add to this a finite element representation of a fibre reinforced plastic patch. This finite element model consisted of 315 of the bonded elements developed in References [2, 3] each of which makes use of the adhesive model described in Section 2. This model allows for the separate responses of the skin, adhesive and the patch as well as for the effects of transverse shear deformation in the skin, adhesive and the patch.

The geometry of the initial patch design is shown in Figure 3. The patch consists of a uniaxial BFRP laminate with the fibres at a direction of 33 degrees to the spar, i.e. in the direction of the maximum principal tensile stress. The patch is stepped in the thickness from one ply to six plies as shown in Figure 3. (A single ply of BFRP is approximately 0·125 mm thick).

Because of the urgent need for the repair and the limited time available for the structural design it was decided to limit the design study to a boron fibre reinforced plastic patch. One of the reasons for the use of boron and not carbon is that the coefficient of thermal expansion of boron is closer to that of aluminium than is the coefficient of expansion of carbon, which can in fact be negative for certain lay-ups. In addition the modulus of boron (e.g. 208 GPa) is significantly greater than that of carbon (e.g. 140 GPa).

The boron was considered as being bonded to the aluminium wing skin with an epoxy nitrite adhesive. The material properties of the BFRP used in the study were

$$E_{11} = 208 \text{ GPa}$$

$$E_{22} = 25{\cdot}4 \text{ GPa}$$

$$\nu_{12} = 0{\cdot}1677$$

$$\nu_{21} = 0{\cdot}0205$$

$$G_{12} = 7{\cdot}23 \text{ GPa}$$

$$G_{13} = 7{\cdot}23 \text{ GPa}$$

$$G_{23} = 4{\cdot}94 \text{ GPa}$$

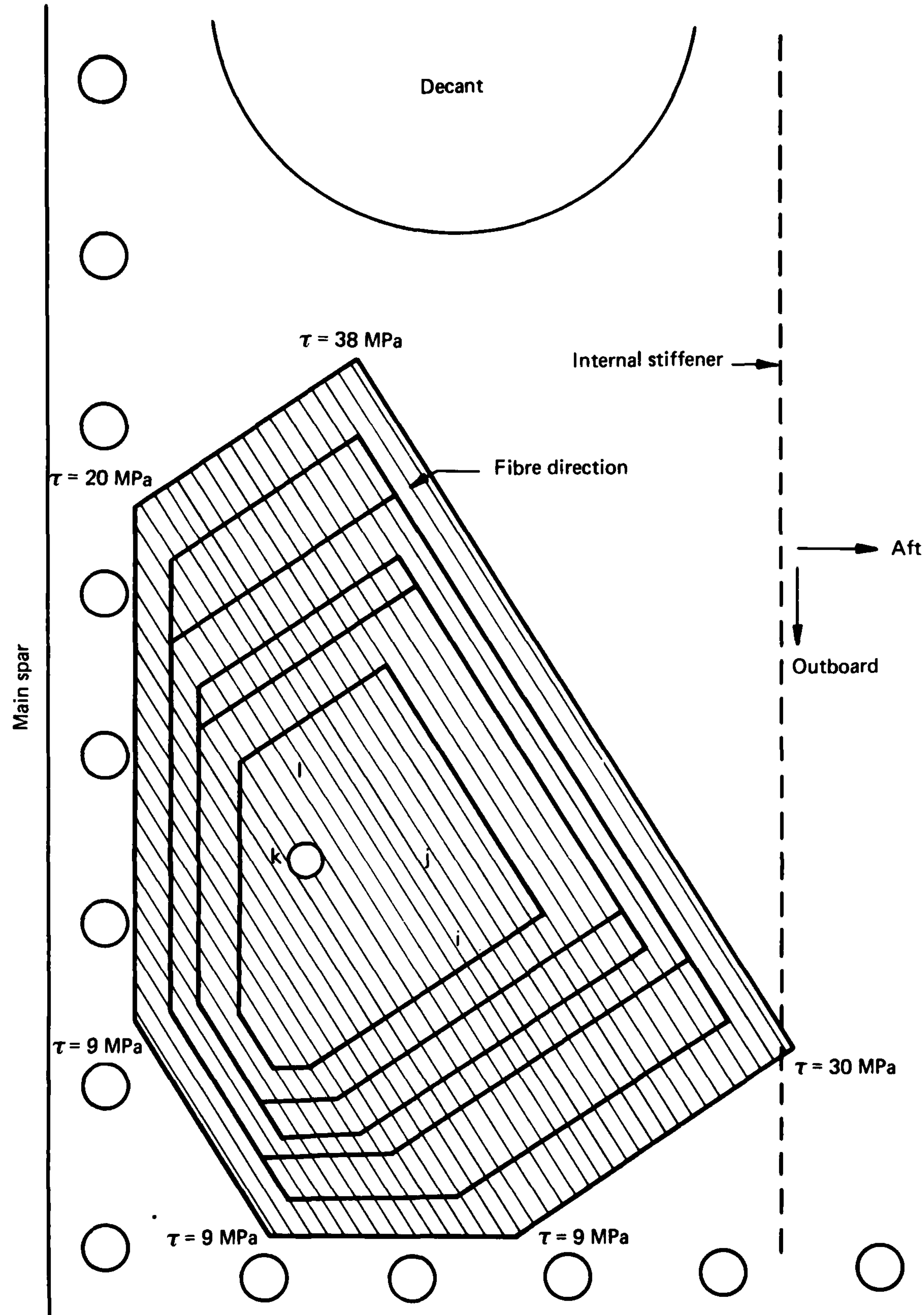

FIG. 3 INITIAL A.R.L. DESIGN OF FGRP PATCH FOR MIRAGE WING SKIN (Full Scale)

which are for a unidirectional boron epoxy laminate with the:

1 axis in the direction of the fibres

2 axis perpendicular to the fibres

3 axis in the thickness direction

The shear modulus of the epoxy nitrite adhesive was taken to be $G_a = 0 \cdot 965$ GPa while the Young's modulus and Poisson's ratio of the wing skin were taken as $E = 71 \cdot 0$ GPa and $\nu = 0 \cdot 32$ respectively.

Before presenting the results of this study it is necessary to discuss the design criteria which will ultimately be used to decide on the final patch design. The basic criterion used was that the patch must reduce the maximum stresses at the fairing hole and the associated rivet holes, see Figure 1, to the same level as in the wing skin some distance from the hole. As this representative stress level, the stresses at a point labelled **B** in Figure 1 were chosen at limit load. This corresponds to a flight manoeuvre load of 7·5 g. The principal stresses at this point are

$$\sigma_1 = 159 \text{ MPa}, \quad \sigma_2 = -79 \text{ MPa}$$

In addition to the above design requirement it is important to note that a fractographic investigation [8] of the crack at the fairing hole attachment hole in the Swiss test had revealed that the crack commenced to grow some time before 1000 flights had been applied (i.e., very early in the test). As a result it must be assumed that there will be small cracks already in either the fairing hole or in a rivet hole. Consequently, the patch will not be designed primarily to increase the time to crack initiation. On the contrary the prime purpose of the patch will be to reduce the rate of crack growth. This is best done by reducing the maximum principal stress in the direction perpendicular to the direction of crack growth. In addition the patch itself must satisfy the two design constraints enunciated in [6], namely that at the maximum limit load of 7·5 g.

(1) The maximum fibre strain must not exceed 0·005. This is equivalent to a fibre stress of 1000 MPa.

(2) The maximum shear stress in the adhesive must not exceed 45 MPa, otherwise fatigue damage to the adhesive will occur.

Having thus decided on our design limitations let us now consider five different patches all of which have the same general geometrical shape, and stepping as shown in Figure 3. These patches may be divided into two distinct groups: a group of three in number which have a hole in the patch so as to allow for the fairing attachment, and the remaining two patches which have fibres covering the fairing hole. Of the fiive patches three are unidirectional patches (which we will abbreviate as u.d.) with the fibres at 33 degrees to the spar and two consist of a balanced lay-up of four layers of boron at an angle of 33 degrees to the spar and two layers perpendicular to these four layers. (This lay-up we will denote by 0/90.) Note that if the problem had been one of merely delaying crack initiation other patch lay-ups would have been considered.

The effects that these patches have on the panel stresses, at limit load, is shown in Table 2.

Even at limit load we see that in all of the patches the adhesive shear stress is below the value of 45 MPa and as a result at no stage should fatigue damage occur in the adhesive. We also see that of the five patches considered the two unidirectional patches (numbers 1 and 4) of thickness 0·762 mm best reduce the maximum stress σ_1 at the fairing hole and at the two rivet holes. Indeed they both reduce stress fields in the vicinity of the holes to values similar to the stress field at the reference point B. Of these two patches, patch 4 is at first glance the most desirable since the maximum stress developed in the fibres in patch 4 is almost half that developed in patch 1. This is due to the fact that patch 4 contains no hole and, as a result, does not allow for attachment of the fairing at this point. However, since at limit load the maximum stresses in patch 1 result in a fibre strain of 0·004, which is below the maximum permissible working strain of 0·005, and since the RAAF wished to retain the fairing attachment hole, patch number 4 was rejected. The patch finally decided upon was therefore patch number 1.

8. N. T. Goldsmith, Fractographic examinations relevant to the F + W Mirage fatigue test. ARL Materials Tech. Memo. No. 371, August 1978.

TABLE 2

Design Study: 7·5 g Load Case

	Hole uncovered			Hole covered	
Patch thickness	0·762 mm	0·635 mm	0·762 mm	0·762 mm	0·762 mm
Lay up	u.d.	u.d.	0/90	u.d.	0/90
Patch no.	1	2	3	4	5
Principal Stresses (MPa) at Locations					
1:					
σ_1	165	175	185	161	181
σ_2	−44	−43	−31	−45	−33
2:					
σ_1	171	182	190	104	184
σ_2	−80	−80	−69	−79	−69
3:					
σ_1	174	186	191	161	180
σ_2	−74	−74	−63	−75	−63
4:					
σ_1	160	169	178	145	166
σ_2	−56	−55	−44	−58	−46
5:					
σ_1	163	170	179	153	173
σ_2	−88	−88	−80	−86	−79
6:					
σ_1	156	165	175	152	171
σ_2	−52	−51	−44	−52	−44
Maximum Stresses in fibres (MPa)					
σ_1	842	880	635	419	320
σ_2	−14	−14	−26	−42	−150
Maximum adhesive shear stress (MPa) at:					
1. Fairing hole	24	24	23	20	20
2. Along edges	38	38	38	38	38
Principal stresses at B (MPa)					
σ_1	155	156	155	155	155
σ_2	−78	−79	−68	−69	−68

Let us now examine the effect of patch number 1 in more detail. The shear stress distribution in the adhesive along the edges of this patch is shown in Figure 3. As mentioned earlier these stresses are significantly below the levels at which fatigue damage occurs in the adhesive. As a result it is unlikely that the patch will debond from the wing skin. The reductions in the maximum principal stresses and the maximum principal strains in the wing skin at locations *i*, *j*, *k* and *l*, as shown in Figure 3, are given in Table 3.

TABLE 3

Stress and Strain Reductions in Wing Skin After Patching

Location	% reduction in max. principal stress and strain	
	Strain	Stress
i	26	32
j	30	34
k	30	35
l	28	33

From this Table we see that the reduction in the strain is not as great as the reduction in the stress. This is due to the fact that the patch is unidirectional and as a result has a greater effect on σ_1 than σ_2. We also see that there is an increase in the effectiveness of the patch as one proceeds from the edges of the patch towards the centre of the patch.

Summarising these results we find that the unidirectional boron fibre patch of thickness 0·762 mm adequately satisfies all of the design requirements and in addition, as required by the RAAF, still allows for the fairing attachment hole to be retained.

4. REPAIR OF THE DRAIN HOLE CRACKS

Shortly after the BFRP patch for the fairing attachment hole had been designed cracks were found, in service aircraft, in the drain hole region slightly inboard of the fairing attachment hole (see Fig. 1). ARL was again tasked with the development of a BFRP patch for this area. After consultation with the RAAF it was decided that the patch be developed for installation in the field. Because of the significance of the cracking and the long life required of the repair a considerable amount of research was required before the repair could be implemented.

This paper deals with the structural design of the repair. Other aspects of the repair program are contained, for example, in the paper by Baker *et al.* [1].

As mentioned above cracks were found in the drain hole region in a number of Mirage aircraft in service with the RAAF. These cracks were predominantly found at an angle of 45 degrees to the main spar. To initially investigate the feasibility of a BFRP repair it was decided to undertake a design study into the repair of a crack whose tips were 111 mm apart and which lay at 45 degrees to the spar (see Fig. 4). In fact this crack was a model of the longest crack which had yet reached towards a bolt hole. Cracks which had reached a bolt hole were to be repaired in an entirely different manner and as a result are not considered in this report.

As a first step in the design of the repair a study of the cracked, but unpatched, region was undertaken. A detailed finite element model of the area surrounding the drain hole region was developed, see Figure 5. This contained the crack, described above, and which used the special crack tip elements developed by the authors in References [8, 9]. The loads applied to this model were obtained directly from the stress distribution which resulted from the finite element model described in Section 3 and which correspond to the 7·5 g load case.

This study gave the values of the stress intensity factors to be $k_1 = 72\ \mathrm{MPa}\sqrt{m}$ and $k_2 = 3{\cdot}3\ \mathrm{MPa}\sqrt{m}$ at the tip closest the spar and $k_1 = 68\ \mathrm{MPa}\sqrt{m}$, $k_2 = 0{\cdot}5\ \mathrm{MPa}\sqrt{m}$ at the tip closest to the root rib. These values are consistent with a fractographic examination of the crack which showed that the crack was essentially growing as a mode I fracture and that of the two crack tips the tip closest to the spar was growing the fastest. Indeed the tip closest to the spar was found to be very close to final failure.

Having thus obtained a reasonable model for the unpatched crack we add to this a finite element representation of the repair. Six BFRP patch configurations were considered, each with the same plan form, see Figure 4. Each patch was modelled using approximately 380 of the "bonded" elements previously described.

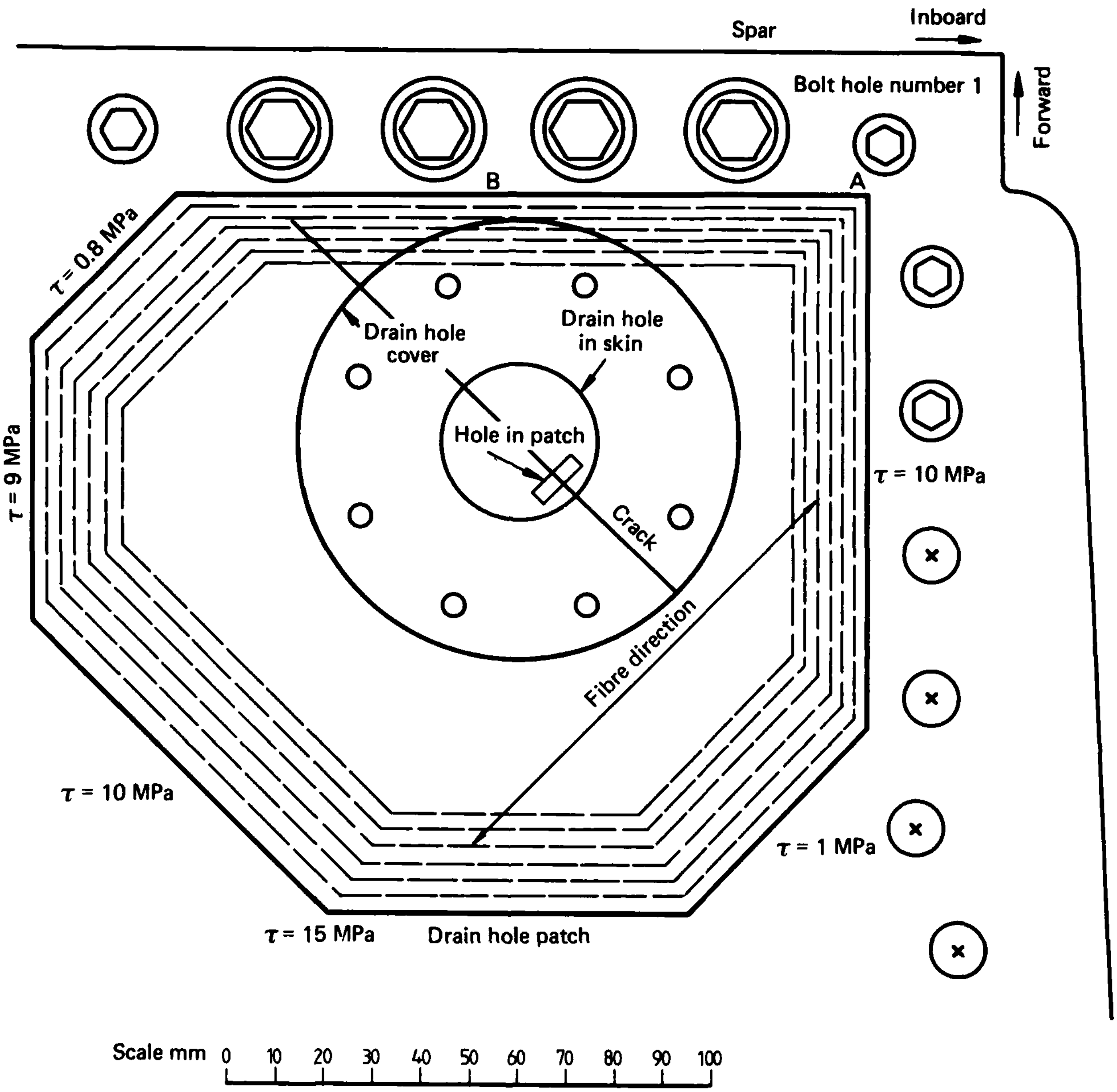

FIG. 4 GENERAL ARRANGMENT OF PATCHES FOR DRAIN HOLE

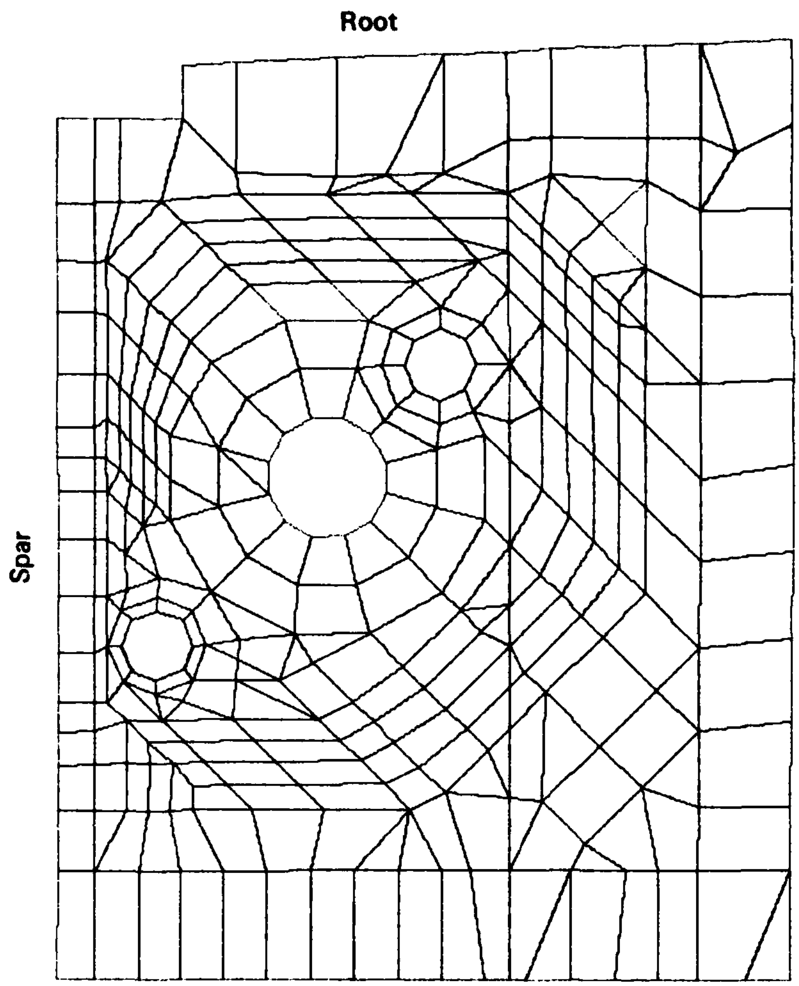

FIG. 5 FINITE ELEMENT MESH FOR THE DRAIN HOLE REGION

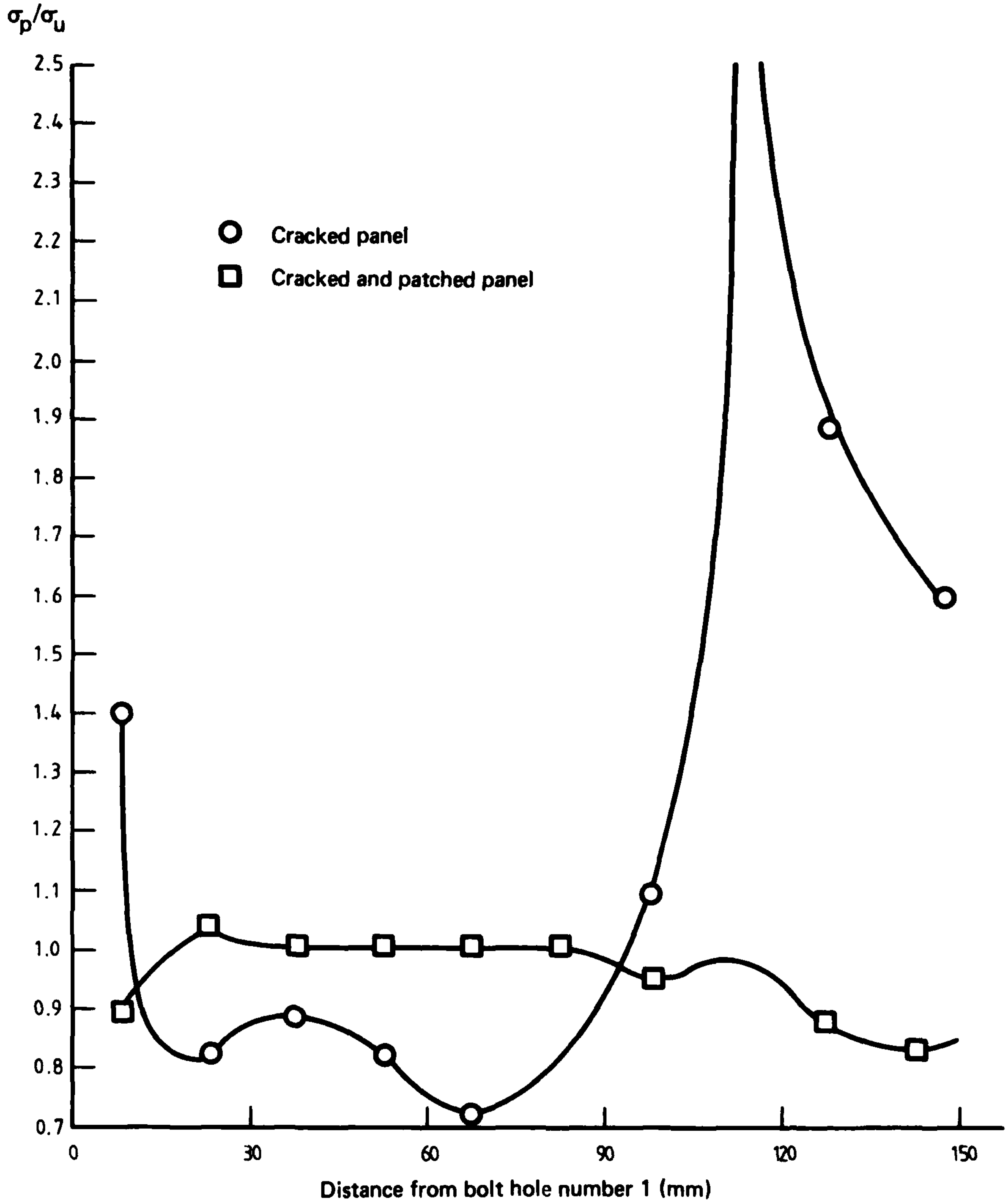

FIG. 6 EFFECT OF PATCH OF SKIN STRESSES

All of the six patches considered are unidirectional laminates and are internally stepped, i.e., with the longest ply on the outside. The fibre direction is at ninety degrees to the crack.

Initially it was uncertain if carrying the fibres over the drain hole was necessary, or how frequently the drain hole was used in service. As a result, in three of the patches considered a hole was left so as not to interfere with the draining of the wing. In the other three patches varying amounts of the hole were covered. In one case one third of the total area of the hole was covered while in the other two cases virtually all of the hole was covered.

For each of the patches the maximum shear stresses in the adhesive bonding the patch to the wing skin occurred at points A, B, C and D (see Fig. 4) The maximum stresses in the fibres occurred at point D for the patches with a hole in the patch, and in the fibres over the hole in the patches with the hole partially covered. The values for these stresses, along with the percentage reduction of the stress intensity factor k_1 at each tip, achieved by each patch are shown in Table 4. Here k_{1u} and k_{1p} are the values of the stress intensity factors before and after patching respectively.

Here we see that all of the six patches achieve a reduction in the stress intensity factor k_1 of at least 91%. Consequently they would all significantly retard crack growth. Similarly for all of the patches the fibre strains are below the maximum working level of 0·005, which corresponds to a stress of 1000 MPa, although of the six patches numbers 5 and 6 have by far the greatest factors of safety. As a result the patch design was finally chosen primarily on the basis of the magnitude of the shear stresses developed in the adhesive. On this basis patch numbers 1, 2, 3, and 4 may be rejected. The two remaining patches are patch numbers 5 and 6. Of the two, Table 3 shows that the adhesive shear stresses along the edges of the patch, are substantially higher for patch number 5 than for patch number 6, although both are below the threshold value for fatigue damage. As a result patch 6 is much less likely to suffer fatigue damage to the adhesive bond. Hence patch number 6 was adopted as the final repair.

Consulting Table 4 we see that at locations C and D in patch 6 the shear stress in the adhesive is sufficiently high so as to cause concern over the possibility of fatigue damage occurring in the adhesive. However these high values occur in the interior of the patch at the intersection of the crack with the drain hole, and are very localized. As a result any damage which does occur should not spread and, as shown in [6], should have virtually no effect on the stress intensity factors at the crack tips or on the fibre stresses.

Let us now examine patch 6 in more detail paying particular attention to the effect it has on the spar. In Figure 6 is shown the ratio of the maximum principal stress σ_p in the skin panel, along the line of attachment to the spar, for the case when the panel is either cracked and patched or cracked and unpatched, to the maximum principal stress σ_u at corresponding locations in the uncracked panel. From this figure we see that the patch removes the peaks in the stress distribution in the skin in the vicinity of the spar. Indeed the stress distribution in the patched panel is very similar to that in the uncracked panel.

5. THERMAL CONSIDERATIONS

Let us now consider the effect that the difference between the coefficients of thermal expansion of the boron patch and aluminium alloy wing skin has on the residual stresses left in the skin after the patch has been applied. Patching the skin involves heating the area to be patched to approximately 120°C. The patch which has also been heated to 120°C, is then attached and the patched structure is allowed to cool to ambient temperature. It is during this cooling phase that the difference in the coefficients of expansion between the patch, $\alpha_1 = 4 \cdot 5 \times 10^{-6}$ per °C and $\alpha_2 = 20 \times 10^{-6}$ per °C, and the wing skin, $\alpha = 23 \times 10^{-6}$ per °C, causes a residual thermal stress to be left in the structure. (Note that α_1 is the coefficient of expansion in the fibre direction and α_2 is that perpendicular to the fibre direction.)

In order to analyse this phenomenon the shear modulus of the adhesive was taken as zero at 120°C and was assumed to increase linearly, as the temperature decreased, to a value of 0·965 MPa at ambient temperature i.e. 40°C. At each step decrease in temperature the adhesive layer was modelled using the finite element method described in Section 2. As a result of this analysis it was found that, when the skin was assumed to be restrained from in plane movement by the spar and root rib attachments, the mean residual stress left in the skin under the patch

TABLE 4

Effect of Drain Hole Patch; 7·5 g Load Case

Patch Number	1	2	3	4	5	6
Maximum Patch Thickness (mm)	0·762	0·762	0·762	0·889	0·889	0·889
Adhesive Thickness (mm)	0·102	0·102	0·102	0·203	0·203	0·203
Thickness of First Layer (mm)	0·127	0·254	0·127	0·254	0·254	0·127
Covering of Drain Hole	open	open	1/3 covered	open	substantially covered	substantially covered
Adhesive Shear Stress (MPa) at points:						
A	29	43	29	31	26	18
B	55	79	55	58	42	30
C	181	179	164	120	63	64
D	153	153	131	98	50	51
Maximum Fibre Stress (MPa)	953	930	760	911	450	455
Reduction in Stress Intensity Factor k_1, i.e. $1-k_{1p}/k_{1u}$, at:						
1. Spar Tip	91%	91%	91%	91%	92%	91%
2. Root Rib Tip	99%	99%	99%	99%	99%	99%

was a tensile stress of 8·7 MPa. This stress should not significantly alter fatigue behaviour of the patched panel.

For a more detailed discussion of the effects of thermal mismatch the readers are referred to References [9, 10]. Further information of the use of fibre composite repair schemes is contained in [11].

6. CONCLUSION

This paper has outlined the basic steps in the design of the two BFRP patch repairs for the wing skins of Mirage aircraft. The proposed six layer patch for the fairing attachment hole region should prevent the development of cracks in that region while the proposed seven layer patch for the drain hole region should prevent the growth of cracks measuring as much as 111 mm tip to tip. However a considerable amount of experimental work is also being done to validate the patch designs and this will be reported elsewhere.

---

9. R. Jones, and R. J. Callinan, Thermal considerations in the patching of metal sheets with composite overlays, J. Struc. Mechanics, 8, 2, 1980 (In press).
10. A. A. Baker, G. A. Hawkes, and E. J. Lumley, Fibre Composite Reinforcement of Cracked Aircraft Structures, Thermal Stress and Thermal Fatigue Studies, Proceedings 2nd Int. Conf. in Composite Materials, Toronto, Canada, April 1978 (In press).
11. A. A. Baker, A summary of work on applications of advanced fibre composites at the Aeronautical Research Laboratories, Australia, Composites 9, 11–16, 1978.

DISTRIBUTION

	Copy No.
AUSTRALIA	
Department of Defence	
Central Office	
Chief Defence Scientist	1
Deputy Chief Defence Scientist	2
Superintendent, Science and Technology Programs	3
Australian Defence Scientific and Technical Representative (UK)	—
Counsellor, Defence Science	—
Joint Intelligence Organisation ([redacted])	4
Defence Library	5
Document Exchange Centre, D.I.S.B.	6–22
Aeronautical Research Laboratories	
Chief Superintendent	23
Library	24
Superintendent Division — Structures	25
Divisional File — Structures	26
Authors: R. Jones	27
R. J. Callinan	28
B. C. Hoskin	29
Materials Research Laboratories	
Library	30
Defence Research Centre, Salisbury	
Library	31
Central Studies Establishment	
Information Centre	32
Engineering Development Establishment	
Library	33
RAN Research Laboratory	
Library	34
Defence Regional Office	
Library	35
Navy Office	
Naval Scientific Adviser	36
Army Office	
Army Scientific Adviser	37
Air Force Office	
Aircraft Research and Development Unit, Scientific Flight Group	38
Air Force Scientific Adviser	39
Technical Division Library	40
D.G. Air Eng.-AF	41
HQ Support Command (SENGSO)	42
RAAF Academy, Point Cook	43

Department of Productivity	
Government Aircraft Factories	
Manager/Library	44
Department of Transport	
Secretary	45
Library	46
Airworthiness Group, Mr K. O'Brien	47
Statutory, State Authorities and Industry	
CSIRO, Mechanical Engineering Division, Chief	48
Qantas, Library	49
Trans Australia Airlines, Library	50
Ansett Airlines of Australia, Library	51
Commonwealth Aircraft Corporation, Library	52
Hawker de Havilland Pty. Ltd.:	
Librarian, Bankstown	53
Manager, Lidcombe	54
CANADA	
CAARC Coordinator Structures	55
NRC, National Aeronautical Establishment, Library	56
NRC, Division of Mechanical Engineering, Director	57
FRANCE	
AMD-BA (Mr M. Peyrony)	58
INDIA	
CAARC Co-ordinator Materials	59
CAARC Co-ordinator Structures	60
National Aeronautical Laboratory, Director	61
INTERNATIONAL COMMITTEE ON AERONAUTICAL FATIGUE	
per Australian ICAF Representative	62–86
NETHERLANDS	
National Aerospace Laboratory (NLR), Library	87
NEW ZEALAND	
Transport Ministry, Civil Aviation Division, Library	88
Librarian, Defence Scientific Establishment	89
SWITZERLAND	
F + W	
Mr L. Girard	90
Dr R. Kaelin	91
UNITED KINGDOM	
Aeronautical Research Council, Secretary	92
CAARC, Secretary	93
Royal Aircraft Establishment, Farnborough, Library	94
CAARC Co-ordinator, Structures	95
British Aerospace Corporation:	
Kingston-Brough, Library	96
Manchester, Library	97
Kingston-upon-Thames, Library	98
Hatfield-Lostock Division	99
Hatfield-Chester Group	100

LMED

8